Parameter development for near-fully dense LPBF-produced stainless steel 316 using a design of experiment approach

Marné van Niekerk[1,2*], *James* Dicks[2], *CP* Kloppers[1], and *Thorsten Hermann* Becker[2]

[1]Department of Mechanical Engineering, North West University, South Africa
[2]Centre for Materials Engineering, University of Cape Town, South Africa

Abstract. This study aims to develop parameters that minimize porosity in SS316 using a Design of Experiments approach (DOE). Employing the D-Optimal (D-Optimal) method and ANOVA, we determined a quadratic model for predicting porosity. The model was validated through three-point predictions, demonstrating high accuracy. The study utilised the bootstrapping method to identify the minimum sample size required for reliable predictions, establishing that 15 samples are sufficient. This was verified by plotting three sets of 15 random samples, where actual vs. predicted values showed strong agreement. The study achieved the highest density of 7.94 g/cm³, corresponding to 99.6% relative density. These findings offer a robust framework for optimising material properties to reduce porosity effectively.

1 Introduction

Laser Powder Bed Fusion (LPBF) has transformed manufacturing industries, such as the aerospace, automotive, nuclear, and biomedical sectors, given its ability to produce intricate and high-precision components. While design freedom and complexity are significant advantages of LPBF, the quality of the final component is strongly influenced by the selected printing parameters. The importance of printing parameters was highlighted by Yadroitsev [1], demonstrating that 130 parameters have an effect on the final quality of the part. An important determinant of a final component's quality is the amount of porosity caused during the printing process. Porosity in LPBF can be categorised into three distinct types, namely, (i) lack of fusion pores that occur under conditions of insufficient volumetric energy density (VED), (ii) balling that ensues under too high solidification rate, and (iii) keyhole pores that may result from excessive VED causing evaporation [2]. Attaining near-fully dense components is essential for ensuring optimal mechanical properties and structural integrity since it is generally the initial stage in LPBF manufacturing [3, 4]. However, identifying printing parameters that result in near full density can be challenging owing to the wide design space and parameter selection. The influence of laser power (P), layer thickness (t), hatching distance (h) and scan speed (v) on porosity is most commonly investigated in LPBF

* Corresponding author: marne.vanniekerk@nwu.ac.za

[2]. These four parameters are typically characterised as VED and expressed through equation 1, which is the amount of energy exerted onto a volumetric unit of powder [4].

$$VED = \frac{P}{(v \times h \times t)} \quad (1)$$

In order to minimise porosity, a processing map methodology for developing printing parameters in LPBF has been developed, which uses a surface contour plot of laser power and scanning velocity alongside critical lines that differentiate the processing regimes, as illustrated in Figure 1 [5, 6]. These windows provide a visual guide for achieving near-fully dense parts while recommending specific process parameter combinations to avoid defects or improve melt pool adhesion [7].

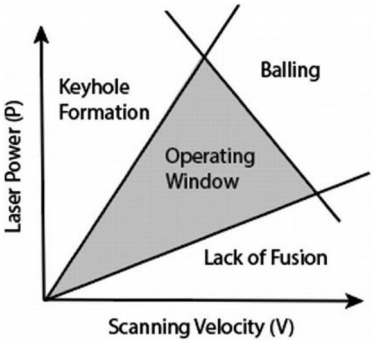

Fig. 1. Processing window as reconstructed from Metal Additive Manufacturing Processes – Laser and Electron Beam Powder Bed Fusion [6].

Creating processing maps through experimental characterisation can be expensive and time-consuming, requiring large experimental matrices. Therefore, it is of value to obtain the maximum amount of information from the minimum number of experimental sample points. As a result, statistical methods have been increasingly used to reduce the number of experimental sample points. Several fractional factorial and optimal design matrices have been used [8, 9], which can lend themselves to efficient analysis of variance (ANOVA) and response surface method (RSM) analysis to understand parametric influences. For example, Deng *et al.* [10] employed the RSM approach to obtain high density and low surface roughness in LPBF, while Sun *et al*. [9] applied the Taguchi method in addition to ANOVA for analyses on LPBF Ti6Al4V alloy to obtain minimal porosity.

However, investigations into using design of experiments through a statistical approach to minimise sample sizes for parametric modelling is still currently lacking in literature. The D-optimal method is particularly well-suited for creating a design space to minimise LPBF porosity with limited samples [11, 12]. This method enhances the efficiency and precision of the experimental design by providing informative and unbiased estimates of the effects of various printing parameters [11]. It aims to minimise the generalised variance of the parameter estimates, resulting in accurate and reliable conclusions about how each factor influences porosity. Additionally, the D-optimal method allows for a comprehensive exploration of the design space using reduced experimental runs, thereby saving time and resources in optimising LPBF parameters [11]. Furthermore, unlike several other designs of experiments, the D-optimal design allows for an asymmetric design space that can be exploited to align within the processing window while still allowing for orthogonal RSM analysis, which allows for the independent estimation of individual effects of different factors [11]. Stainless Steel 316 (SS316) was chosen as an appropriate material for this study, given that previous studies have been extensively researched into attaining near-full density LPBF-

manufactured SS316 [4, 13, 14]. In a critical review conducted by Gor *et al.*[4] the effect of processing parameters on mechanical properties, including porosity, was examined. The authors concluded in their review that the range of VED, which yields maximum density, is between 80 J/mm^3 and 105 J/mm^3 for LPBF manufactured SS316 [4]. Due to these well-established parametric windows and understanding of LPBF manufactured SS316, it was chosen as a useful material to reliably investigate a statistical approach to design of experiments for minimising the sample size required to attain near full density components.

2 Methodology

2.1 Material and equipment

Commercially available gas-atomized SS316 powder, supplied by Weartech (Pty) Ltd (Johannesburg, South Africa), was utilised for sample production. The particle size distribution of the powder, as specified in the supplier's datasheet, ranged from 15 to 45 μm, and the chemical composition by weight is detailed in Table 1. Cylindrical samples (10 mm diameter x 15 mm height) were fabricated using the parameters listed in Annexure 1 on a Hyrax machine (Additv Solutions, Pretoria, South Africa) equipped with a 400 W Yb fibre laser featuring a 158 μm spot size. The build chamber was filled with nitrogen to maintain a reductive atmosphere, with the oxygen content regulated to 0.2 vol% (2000ppm) throughout the process.

The machine operates with a linear recoater moving from left to right, and the sample layout was strategically arranged to ensure even powder and heat distribution. Before printing, the powder was dried at 120 °C for three hours and then cooled to 45 °C at a rate of 3 °C/min to ensure minimal moisture content.

The laser power, scan speed, and hatch spacing varied for each parameter combination for each cylindrical sample, as detailed in Table 2. The sample location variation was not considered a significant factor in this study. Moreover, the layer thickness of 0.04 mm, the scanning rotation of 33° between each layer, the stripe scanning strategy, and a laser spot size of 158 μm remained constant.

Table 1. SS316 Chemical Composition [wt.%] as supplied by Weartech.

Element	Fe	Cr	Ni	Mo	Mn	Si	C	S
Standard	bal	16-18	10-14	2-3	≤ 2	≤ 1	≤ 0.03	≤ 0.03
wt%	bal	17.17	10.75	2.53	0.95	0.69	0.01	0.03

Table 2. Factor ranges

Factor	Units	Lower Limit	Higher Limit
Power [A]	W	155	360
Scan Speed [B]	mm/s	800	1800
Hatching Distance [C]	mm	0.063	0.095

Post-manufacturing, the samples were removed from the build plate and milled down, to minimise surface roughness.

2.2 Density measurement

Density measurements of the cylindrical samples were performed at room temperature and atmospheric pressure using the Archimedes method in accordance with ASTM B311. Measurements were taken using an Adam (Johannesburg, South Africa) Luna analytical balance with a sensitivity of 0.0001 g. To minimise the probability of air bubbles forming on the surface of the samples, the samples were milled down using, and acetone was used as the fluid as literature indicates acetone having a lower surface tension than demineralized water. This lower value enables the fluid to better wet the surface minimising the probability of air bubbles to form on the surface [15].

2.3 Design of experiments and analysis

The design space was constructed using the D-Optimal method via the Stat-Ease software, employing a quadratic model. The VED was constrained between 55 and 250 J/mm³. The build comprised 30 samples, including five lack-of-fit points, five replicated points, five centre points as illustrated in the design space in Figure 2.

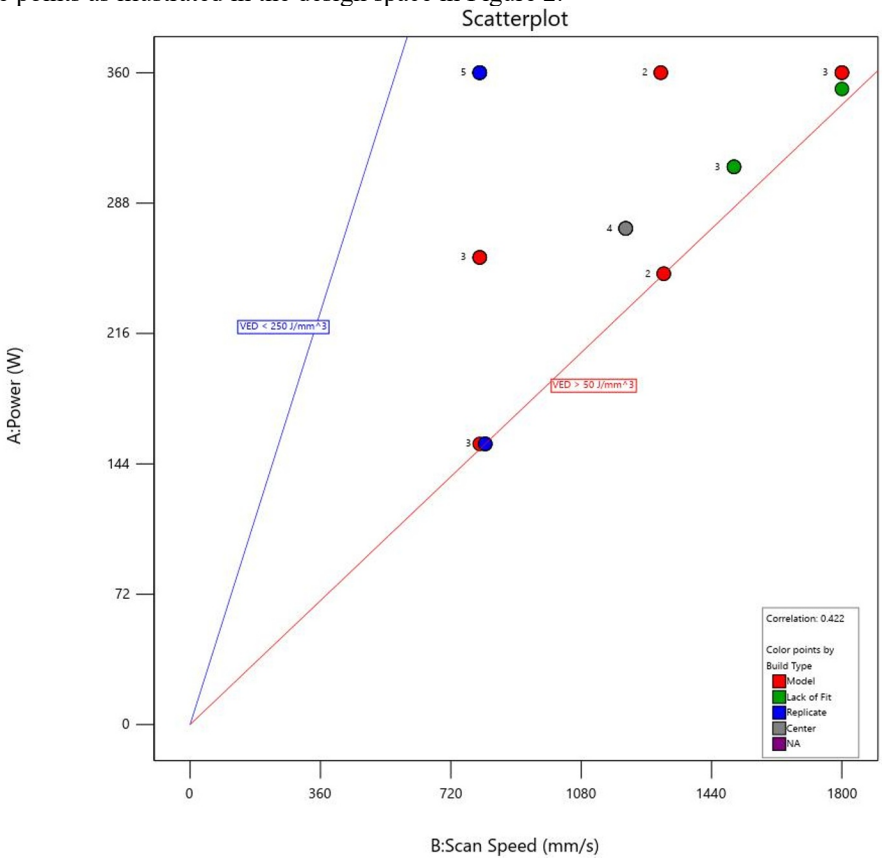

Fig. 2. Design space

The response for each run was then analysed through the software, where a variety of models were applied to the response in order to determine the best fit for the data. The data undergoes analysis via ANOVA, entailing the computation of the sum of squares, degree of freedom (df), mean square, F-value, and p-value. The sum of squares denotes the deviation

of data points from the mean value, while the degree of freedom (df) represents the maximum number of independent values capable of varying within a data sample. Mean square signifies the variance of the data, F-value determines the model's significance, and the p-value quantifies the likelihood of attaining the observed results.

3 Results

The findings of this study provide insights into the use of the statistical method D-Optimal to create a design space for establishing parameters that will minimise porosity. The response (density in g/cm^3) was measured using Archimedes' principle for each run. An ANOVA statistical analysis was conducted on the data, as illustrated in Table 3. Three data points (runs 11, 18, and 28) were excluded as they failed during printing. The fit summary revealed that a quadratic model was statistically significant for the density. The ANOVA results showed that the model had an F-value of 12.78, indicating its significance with a 0.01% chance that the F-value could occur due to noise. A p-value less than 0.05 indicates a significant model term. In this case, A and A^2 are considered significant model terms. A p-value greater than 0.1 indicates that the model term is not significant. Many terms were found to be not significant, suggesting that a model reduction may improve the model. Model reduction can be achieved by applying the p-value criterion, Bayesian information criterion (BIC), adjusted R^2 criterion, or the Akaike information criterion (AICc). The p-value criterion removes terms with a p-value larger than 0.1, while BIC and AICc remove terms to minimize the AIC or BIC value, and the R^2 criterion removes terms that reduce the overall adjusted R^2. After applying each criterion, the terms B, AB, AC, BC, B^2, and C^2 were unanimously removed.

Table 3. Analysis of variance result for Density

Source	**Sum of Squares**	**df**	**Mean Square**	**F-value**	**p-value**
Model	0.3329136	9	0.03699	12.77697	< 0.0001
A-Power	0.0396702	1	0.0396702	13.70260	0.0102
B-Scan Speed	0.0051196	1	0.00511957	1.768366	0.2833
C-Hatching	0.0128768	1	0.012877	4.447846	0.0127
AB	0.002392	1	0.002392	0.826327	0.4514
AC	0.0041824	1	0.004182	1.444688	0.0468
BC	0.0008783	1	0.0008783	0.303393	0.7187
A^2	0.0362774	1	0.036277	12.5307	0.0169
B^2	0.001516	1	0.001516	0.52366	0.5383
C^2	4.0135e-06	1	4.013532e-06	0.0013863	0.8407
Residual	0.0492	17	0.002895		

Lack of Fit	0.0434877	10	0.00435	5.3137662	0.0871
Pure Error	0.0057288	7	0.00082		
Cor Total	0.38213	26			

The adjusted and predicted R^2 values are used to assess the significance of removing terms on the model's overall performance. Table 4 displays the adjusted and predicted R^2 values, as well as their difference. A difference of less than 0.2 between the adjusted and predicted R^2 is indicative of a good fit. In this case, the original and modified models show differences of 0.1828 and 0.064, respectively, suggesting that neither model is overfit. However, there is a 64.9% reduction in the difference between the adjusted R^2 and predicted R^2, indicating that the modified model is likely to offer a better fit to the data. The modified model has removed the terms, as detailed in Table 5 below.

Table 4. Original and modified model's R^2 values

Original/Modified	**R^2**	**Adjusted R^2**	**Predicted R^2**	**Difference**
Original	0.8712	0.803	0.6202	0.1828
Modified	0.8348	0.8132	0.7492	0.064

Table 5. Original and modified model's terms included or removed

Terms	**A**	**B**	**C**	**AB**	**AC**	**BC**	**A^2**	**B^2**	**C^2**
Original	X	X	X	X	X	X	X	X	X
Modified	X		X				X		

The original and modified models show minor differences in their ability to predict data points. This is evaluated by plotting predicted versus actual data, with ideal predictions falling on the 45° line. In Figure 3, two graphs are depicted: the original model correctly predicted three points, whereas the modified model accurately predicted four points, with one point overlapping. Considering this, the modified model is slightly more accurate than the original model.

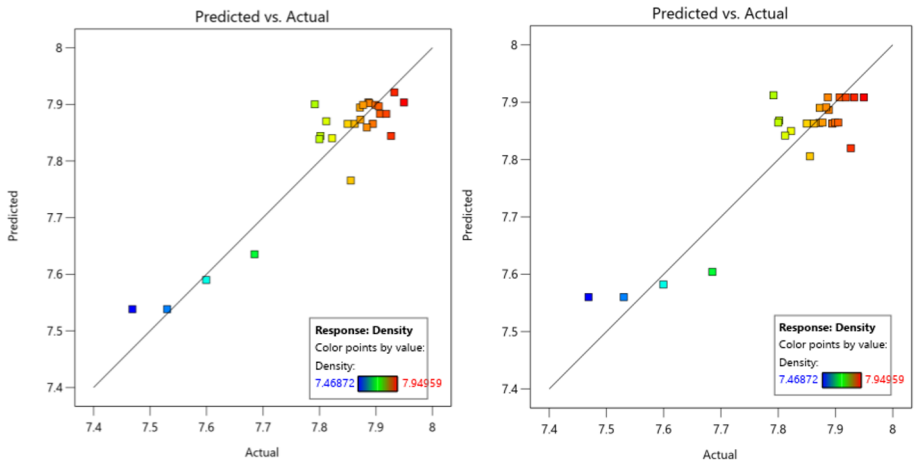

Fig. 3. Left: Original model Predicted vs Actual, Right: Modified model Predicted vs Actual

To confirm this, 3 verification points were conducted using samples with the parameters listed in Table 5. Table 6 depicts the original and modified model's prediction and confidence interval (CI).

Table 5. Verification points' parameters

Sample Number	Power [W]	Scan Speed [mm/s]	Hatch distance [mm]
1	360	1700	0.079
2	360	1400	0.063
3	360	1600	0.063

Table 6. Original and modified model's outputs

Sample	Analysis	Predicted	Actual	Difference	95% CI low	95% CI high
1	Original	7.8759	7.9226	0.0467	7.81148	7.94029
	Modified	7.8845		0.0381	7.85377	7.91916
2	Original	7.9182	7.9000	0.0182	7.83696	7.99943
	Modified	7.90848		0.0048	7.86826	7.9487
3	Original	7.90519	7.9132	0.008	7.81855	7.95697
	Modified	7.90848		0.0047	7.86826	7.9487

The data for both models fall within the confidence interval. However, as indicated in Table 6, the modified model demonstrates superior accuracy in predicting the data. The coefficients for each term are delineated in Table 7 and can be utilised to forecast the density.

Table 7. Factors for original and modified model.

Coded Model for Density		
Original	Modified	
7.180825056	6.8937	Intercept
0.005627	0.006718	Power
-0.000029		Scan Speed
-3.63497	-1.37595	Hatching
1.05×10^{-6}		Power × Scan Speed
0.014015		Power × Hatching
-0.001259		Scan Speed × Hatching
-0.000012	-0.00001	Power²
-1.12×10^{-7}		Scan Speed²
-3.41995		Hatching²

4 Discussion

4.1 A systematic approach to optimising process parameters to achieve near-full density in SS316 L

A D-Optimal Design of Experiments (DoE) with a quadratic model was selected to determine process parameters that will minimise porosity. Based on the literature, the VED where minimal porosity is typically obtained in SS316 ranges from 80-120 J/mm³ [14]. However,

to increase the response surface's surface area, it was decided to broaden the VED range and set it between 55 J/mm³ and 250 J/mm³. The ranges for power, scan speed, and hatch distance, as described in Section 2.2, further constrained the design space, providing a non-symmetrical design space.

By analysing the responses of the 27 valid data points, the study was able to investigate the effects of power, scan speed, and hatch distance on density. The ANOVA table indicated that hatch spacing and power significantly contribute to the density of the samples, with an F-value of 13.7 and 4.45, respectively. This is also illustrated through the interaction plot in Figure 4 below, where non-parallel lines indicate interaction on the response.

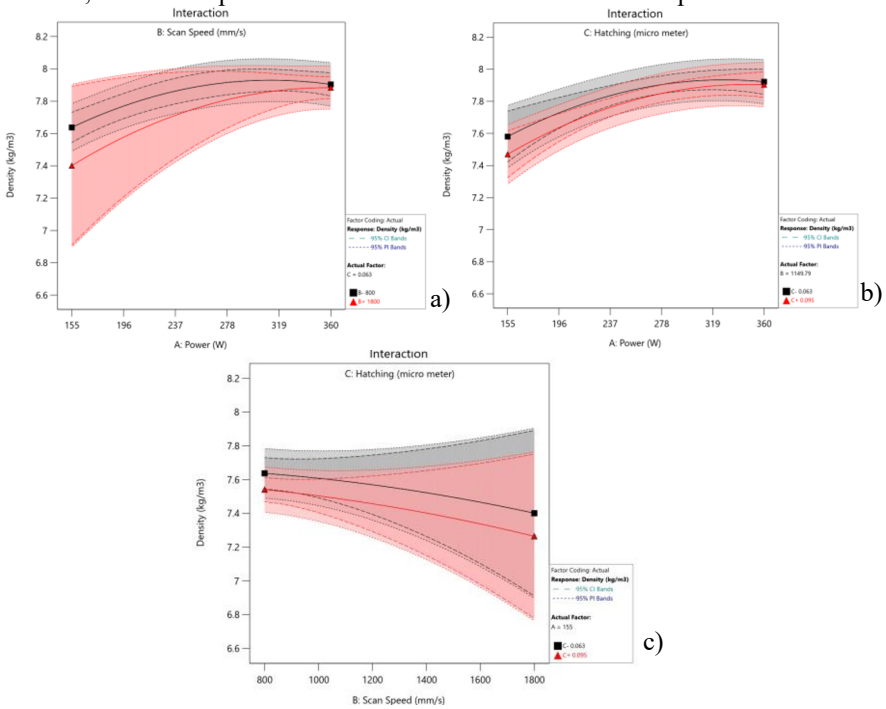

Fig. 4. a) Interaction between scan speed and power, b) interaction on hatching distance and power, c) interaction between hatching distance and scan speed.

As seen in the contour maps in Figure 5, lower hatch distance values and higher power values result in higher porosity. This study calculated the highest density as 7.949 g/cm³ at a power of 360W, scan speed of 800 mm/s, and hatch distance of 0.063 mm. If we were to take the standard density of SS316 as 7.98 g/cm^3 , a relative density of 99.61%.

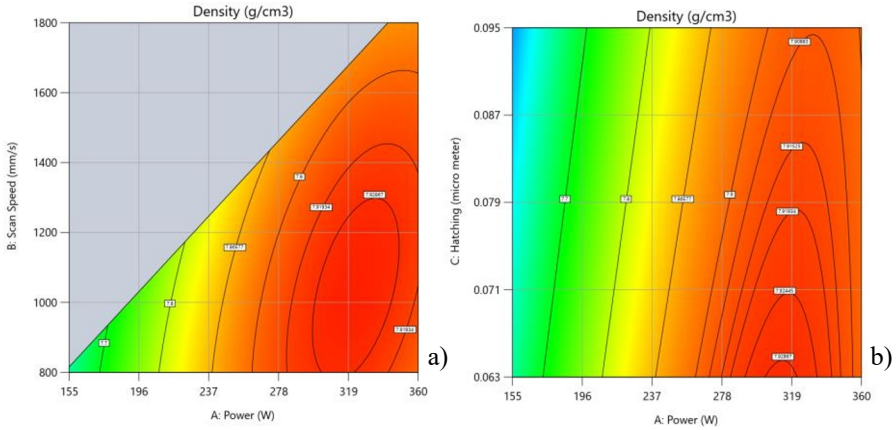

Fig. 5. a) Contour plot of power vs scan speed, b) contour plot of Hatch spacing and power.

4.2 Determine the minimum number of samples required to establish printing parameters that provide near-full density in SS316 LPBF components

To find the minimum sample size needed, a statistical technique called Bootstrapping can be used. This method involves creating multiple bootstrap samples by resampling from the original data set. These samples are then used to estimate parameters, assess model stability, and determine the required sample size for a given model. In this study, a MATLAB code was written to find the minimum sample size for the modified model. The model accuracy was evaluated by calculating the mean and standard deviation of the bootstrap coefficients and ensuring that they were within a specified tolerance of 0.05 of the predefined coefficients.

Our analysis using bootstrap resampling revealed that a minimum of 15 samples is necessary to maintain the accuracy of our modified quadratic model. This conclusion was drawn by iteratively resampling the data and evaluating the consistency of the model coefficients. Subsequently, we randomly selected 15 data points from the original dataset and applied the model to assess its ability to predict density within a smaller population. As depicted in Figure 6, where each point is coloured to distinguish individual data points. The colours are used solely to enhance visibility and do not represent any specific scale or density value. The model consistently predicted the density with an average R^2 value of 0.8585, an adjusted R^2 value of 0.8349, and a Residual Sum of Squares (RSS) of 0.029, as illustrated in Table 8. These results indicate that 85.85% of the variability in the response can be accounted for by the model, while adjusting for factors explains 83.49% of the variability. The difference between the adjusted R^2 and R^2 values (less than 0.05) suggests that the factors contribute significantly to the prediction of the density.

Table 8. Model fit of Modified model on 15 samples.

	15 Runs #1	**15 Runs #2**	**15 Runs #3**	**Average**
R^2	0.8616	0.8068	0.9071	0.8585
RSS	0.0208	0.0364	0.0298	0.029
Adjusted R^2	0.8386	0.7746	0. 8916	0.8349

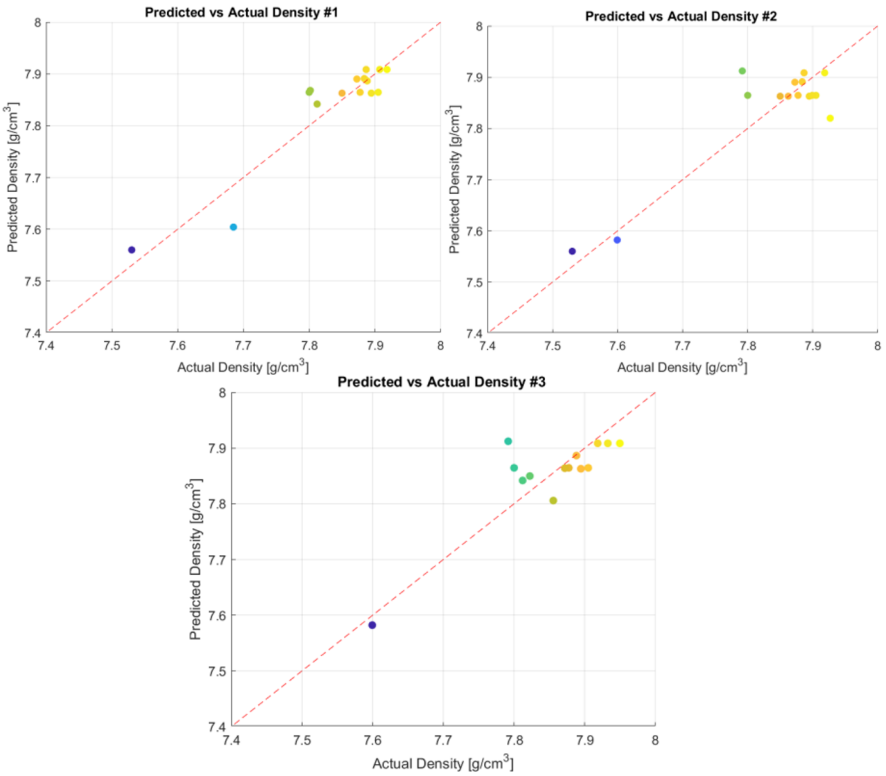

Fig. 6. Modified model prediction on 15 runs

5 Conclusion

This study establishes a systematic approach to optimise process parameters for achieving near-full density in SS316 LPBF components. Utilising Design Expert software and the D-Optimal methodology, we determined the minimum number of samples required to establish printing parameters that yield near-full density. The investigation highlighted the significant influence of power and hatch spacing on the density of SS316 components produced via LPBF. Specifically, a VED range of 74-178 J/mm³ was found to result in a relative density above 99%, with the highest recorded density of 7.94 g/cm³ achieved using parameters of 360W, 800 mm/s, and 0.063 mm. The model's accuracy was validated with 15 samples, confirmed through bootstrapping and actual vs. predicted plotting.

In conclusion, the D-Optimal method is a robust and effective DoE approach for minimising porosity in SS316 LPBF components. This study utilised VED to define the design space; however, future research could explore whether alternative parameter combinations offer superior results. Comparative studies involving other optimisation tools, such as Taguchi or Central Composite Design, could provide insights into their effectiveness and model accuracy. Additionally, verifying the design space through Optical Microscopy (OM) or Scanning Electron Microscopy (SEM) could help identify the types of porosity present in the samples. Future studies might also examine the effect of Particle Size Distribution (PSD) on determining the appropriate VED, potentially reducing the number of samples needed in subsequent research.

The authors of this study would like to thank NWU for their assistance in printing the samples and UCT for their support of the Statistical software Stat Ease.

They would also like to thank the CPAM funding scheme for providing the necessary funding to conduct the study.

6 References

[1] I. Yadroitsev, *Selective laser melting: Direct manufacturing of 3D-objects by selective laser melting of metal powders*, L. L. A. Publishing,

[2] A.B. Spierings, N. Herres, G. Levy, *Influence of the particle size distribution on surface quality and mechanical properties in AM steel parts*, *Rapid Prototyping Journal,* **17**, 195-202 (2011)

[3] H. Gong, K. Rafi, H. Gu, G.D. Janaki Ram, T. Starr, B. Stucker, *Influence of defects on mechanical properties of Ti–6Al–4V components produced by selective laser melting and electron beam melting*, *Materials & Design,* **86**, 545-554 (2015)

[4] M. Gor, H. Soni, V. Wankhede, P. Sahlot, K. Grzelak, I. Szachgluchowicz, J. Kluczyński, *A Critical Review on Effect of Process Parameters on Mechanical and Microstructural Properties of Powder-Bed Fusion Additive Manufacturing of SS316L*, *Materials*, vol. 14, no. 21, doi: 10.3390/ma14216527.

[5] J. Beuth, N. Klingbeil, *The role of process variables in laser-based direct metal solid freeform fabrication*, *JOM,* **53**, 36-39 (2001)

[6] S. Joshi, R. Martukanitz, A. Nassar, P. Michaleris, "Metal Additive Manufacturing Processes – Laser and Electron Beam Powder Bed Fusion," 2023, pp. 59-109.

[7] C. Hou Yi, W. Jianzhao, W. Xinzhi, Y. Wentao, *Process parameter optimization of metal additive manufacturing: a review and outlook*, *Journal of Materials Informatics,* **2**, 16 (2022)

[8] H. Chen, Y.F. Zhao, *Process parameters optimization for improving surface quality and manufacturing accuracy of binder jetting additive manufacturing process*, *Rapid Prototyping Journal,* **22**, 527-538 (2016)

[9] J. Sun, Y. Yang, D. Wang, *Parametric optimization of selective laser melting for forming Ti6Al4V samples by Taguchi method*, *Optics & Laser Technology,* **49**, 118-124 (2013)

[10] Y. Duan, X. Liu, S. Zhang, L. Wang, F. Ding, S. Song, X. Chen, B. Deng, Y. Song, *Selective Laser Melted Titanium Implants Play a Positive Role in Early Osseointegration in Type 2 Diabetes Mellitus Rats*, *Dental Materials Journal,* (2020)

[11] NIST/SEMATECH, *e-Handbook of Statistical Methods*,

[12] S.M.-A. Rudolph, *Near-Beta Titanium Alloys Produced Using Laser Powder-Bed Fusion*, Master of Engineering Masters, Mechanical Engineering, Stellenbosch University, Stellenbosch, South Africa, (2023)

[13] W.M. Tucho, V.H. Lysne, H. Austbø, A. Sjolyst-Kverneland, V. Hansen, *Investigation of effects of process parameters on microstructure and hardness of SLM manufactured SS316L*, *Journal of Alloys and Compounds,* **740**, 910-925 (2018)

[14] N. Ahmed, I. Barsoum, G. Haidemenopoulos, R.K.A. Al-Rub *Process parameter selection and optimization of laser powder bed fusion for 316L stainless steel: A review*, **75**, 415-434 (2022)

[15] T. de Terris, O. Andreau, P. Peyre, F. Adamski, I. Koutiri, C. Gorny, C. Dupuy, *Optimization and comparison of porosity rate measurement methods of Selective Laser Melted metallic parts*, *Additive Manufacturing,* **28**, 802-813 (2019)

7 Annexure 1

Table: Operating parameters

Run	Power (A) [W]	Scan Speeds (B) [mm/s]	Hatch [mm]	Layer Thickness [mm]	VED [J/mm^3]	Density [g/cm^3]
1	274	1200	0.079	0.04	72.26	7.850
2	258	800	0.063	0.04	127.98	7.872
3	351	1800	0.079	0.04	61.71	7.884
4	360	1800	0.063	0.04	79.37	7.907
5	155	800	0.063	0.04	76.88	7.685
6	360	1300	0.063	0.04	109.89	7.933
7	274	1203	0.079	0.04	72.08	7.895
8	258	800	0.095	0.04	84.87	7.927
9	360	1800	0.063	0.04	79.37	7.918
10	249	1300	0.095	0.04	50.40	7.855
11	342	1800	0.095	0.04	50.00	
12	360	800	0.063	0.04	178.57	7.950
13	155	800	0.095	0.04	50.99	7.530
14	360	1800	0.095	0.04	52.63	7.800
15	249	1300	0.063	0.04	76.01	7.822
16	308	1500	0.095	0.04	54.04	7.802
17	274	1200	0.079	0.04	72.26	7.862
18	274	1200	0.079	0.04	72.26	
19	360	1300	0.095	0.04	72.87	7.905
20	274	1200	0.079	0.04	72.26	7.894
21	308	1500	0.079	0.04	64.98	7.873
22	360	800	0.095	0.04	118.42	7.899

23	360	800	0.079	0.04	142.41	7.888
24	155	800	0.079	0.04	61.31	7.599
25	360	800	0.063	0.04	178.57	7.887
26	308	1500	0.063	0.04	81.48	7.792
27	360	800	0.095	0.04	118.42	7.877
28	155	800	0.063	0.04	76.88	
29	155	800	0.095	0.04	50.99	7.469
30	258	800	0.079	0.04	102.06	7.812

8 Annexure 2

MATLAB Code: Bootstrapping

```
% Load data
file = ['Data_Matlab27.xlsx']; %file path
data = xlsread(file, 'SS316', 'B2:G28'); %import data
valid_rows = ~any(isnan(data), 2); %remove invalid data points
data = data(valid_rows, :);

% Define variables
power = data(:, 1); %laser power
speed = data(:, 2); %scan speed
hspacing = data(:, 3); %hatch spacing
density = data(:, 6); %relative density

X = [power, speed, hspacing]; %independent variable matrix
y = density; %dependent variable vector

% Define the predefined model coefficients
intercept = 6.8937;
P_c = 0.006718;
v_c = 0;
h_c = -1.37595;
Pv_c = 00;
Ph_c = 0;
vh_c = 0;
```

```
 P2_c = -0.00001;
 v2_c = 0;
 h2_c = 0;

 % Number of bootstrap samples
 numBootstraps = 1000;
 tol = 0.05; % Tolerance for coefficient comparison

 % Preallocate arrays for bootstrap coefficients
 bootstrapCoeffs = zeros(numBootstraps, 10); % [intercept, P_c,
v_c, h_c, Pv_c, Ph_c, vh_c, P2_c, v2_c, h2_c]

 % Initialize minimum sample size to maximum data size
 minSamples = length(y);

 % Bootstrap resampling
 for nSamples = 10:length(y) % Start with 10 samples and
increase
     for i = 1:numBootstraps
         sampleIndices = randsample(length(y), nSamples, true);
% Bootstrap sample
         Xsample = X(sampleIndices, :);
         ysample = y(sampleIndices);

         % Apply the predefined model to the bootstrap sample
         y_pred_sample = intercept + P_c .* Xsample(:, 1) + v_c
.* Xsample(:, 2) + h_c .* Xsample(:, 3) + ...
                         Pv_c .* Xsample(:, 1) .* Xsample(:, 2)
+ Ph_c .* Xsample(:, 1) .* Xsample(:, 3) + ...
                         vh_c .* Xsample(:, 2) .* Xsample(:, 3)
+ P2_c .* (Xsample(:, 1).^2) + ...
                         v2_c .* (Xsample(:, 2).^2) + h2_c .*
(Xsample(:, 3).^2);

         % Fit a quadratic model to the bootstrap sample
         mdl = fitlm([Xsample(:, 1), Xsample(:, 2), Xsample(:,
3), ...
                      Xsample(:, 1) .* Xsample(:, 2),
Xsample(:, 1) .* Xsample(:, 3), Xsample(:, 2) .* Xsample(:, 3),
...
                      Xsample(:, 1).^2, Xsample(:, 2).^2,
Xsample(:, 3).^2], ysample - y_pred_sample);
```

```
        % Extract and store coefficients
        coeffs = mdl.Coefficients.Estimate;
        bootstrapCoeffs(i, :) = [coeffs(1) + intercept,
coeffs(2) + P_c, coeffs(3) + v_c, coeffs(4) + h_c, ...
                                 coeffs(5) + Pv_c, coeffs(6) +
Ph_c, coeffs(7) + vh_c, coeffs(8) + P2_c, ...
                                 coeffs(9) + v2_c, coeffs(10)
+ h2_c];
    end

    % Calculate the mean and standard deviation of the
bootstrap coefficients
    meanCoeffs = mean(bootstrapCoeffs, 1);
    stdCoeffs = std(bootstrapCoeffs, [], 1);

    % Check if the coefficients are within the tolerance
    if all(abs(meanCoeffs - [intercept, P_c, v_c, h_c, Pv_c,
Ph_c, vh_c, P2_c, v2_c, h2_c]) < tol * stdCoeffs)
        minSamples = nSamples;
        break;
    end
end

% Output the results
fprintf('Minimum sample size to maintain model accuracy:
%d\n', minSamples);
```